ELECTRONIC PROPERTIES
OF SOLID

# Superconducting Current in Hybrid Structures with an Antiferromagnetic Interlayer

**A. V. Zaitsev[a], \*, G. A. Ovsyannikov[a,b], K. Y. Constantinian[a], \*\*, Yu. V. Kislinskiĭ[a], A. V. Shadrin[a], I. V. Borisenko[a], and P. V. Komissinskiy[a,c]**

[a] Kotel'nikov Institute of Radio Engineering and Electronics, Russian Academy of Sciences, Moscow, 125009 Russia
[b] Chalmers Institute of Technology, Göteborg, SE-41296 Sweden
[c] Technische Universität Darmstadt, D-64287, Darmstadt, Germany
*e-mail: zaitsev@hitech.cplire.ru
**e-mail: karen@hitech.cplire.ru
Received August 31, 2009

**Abstract**—It is shown experimentally that the superconducting current density in $Nb/Au/Ca_{1-x}Sr_xCuO_2/YBa_2Cu_3O_{7-\delta}$ hybrid superconducting heterostructures with a $Ca_{1-x}Sr_xCuO_2$ antiferromagnetic (AF) cuprate interlayer is anomalously high for interlayer thicknesses $d_M = 10-50$ nm and the characteristic damping length for superconducting correlations is on the order of 10 nm. The experimental results are explained on the basis of theoretical analysis of a junction of two superconductors (S' and S) connected by a magnetic multilayer with the AF ordering of magnetization in the layers. It is shown that with such a magnetization ordering, anomalous proximity effect determined by the singlet component of the condensate wavefunction may take place. As a result, the critical currents in S'/I/AF/S and S'/I/N/S structures (I denotes an insulator, and N, the normal metal) may coincide in order of magnitude even when the thickness of the AF interlayer considerably exceeds the decay length of the condensate wavefunction in ferromagnetic layers.

**DOI:** 10.1134/S1063776110020172

## 1. INTRODUCTION

The proximity effect in Josephson structures with magnetic interlayers has become the object of intense studies in recent years [1, 2]. The coherence length in oxides is much smaller than in metals, which considerably complicates the preparation of oxide structures with magnetic interlayers. Nevertheless, the anomalous proximity effect in cuprate superconductors was observed in lanthanum-based structures [3] as well as in $Nb/Au/Ca_xSr_{1-x}CuO_2/YBa_2Cu_3O_{7-\delta}$ hybrid heterojunctions [4, 5]. It was reported earlier [6, 7] that the Josephson effect was observed in superconducting cuprate ramp-type junctions with an artificial interlayer with a thickness much larger than the coherence length estimated taking into account the interlayer magnetism. The results obtained in [6] were interpreted in study [7] based on the assumption of interlayer inhomogeneity and the existence of pinholes between superconductors. The percolation mechanism of the superconducting current passing through anomalously thick interlayers was proposed in [8]. However, recent results obtained using a modified technique of cuprate film growth [3–5, 9] cannot be trivially explained by the presence of pinholes. For example, the results of measuring magnetic-field dependences of the critical current in hybrid structures and Shapiro steps oscillating with the intensity of

action at ultrahigh frequencies [4, 5] confirm the existence of the Josephson effect described by the well-known RSJ model [10], which is not observed in the presence of pinholes in the interlayer.

The main attention so far has been paid to analysis of structures with ferromagnetic interlayers [1, 2], while S/AF hybrid structures have not been studied comprehensively. Various aspects of the theory of such structures were discussed in publications [11, 12], in which the antiferromagnet was treated as a structure with atomically thin magnetic layers. It was shown in [12] that the characteristic feature of the Josephson effect in S/AF/S structures is its dependence on whether the number of layers in the antiferromagnet is even or odd. However, some problems (including the possibility of achieving the anomalous proximity effect in the case of diffusive transport of electrons in structures with an AF interlayer) remain unsolved.

Here, we report on the experimental results obtained for 18 chips each of which contains 5 heterojunctions with various areas: $10 \times 10$, $20 \times 20$, ..., $50 \times 50$ μm$^2$. The chips had different thicknesses $d_M$ of the magnetic interlayer and were formed on the basis of epitaxial cuprate superconducting films of $YBa_2Cu_3O_{7-\delta}$ (YBCO) and niobium (Nb) (Fig. 1). The magnetic interlayer (M) was prepared from a
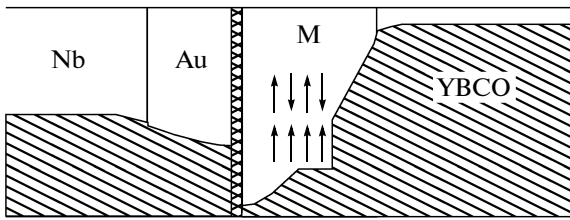
**Fig. 1.** Schematic representation of variation in the condensate wavefunction for heterostructures under investigation. The current is set along the $c$ (horizontal) axis of the structure. The bold line shows the interface between the Au film and the M interlayer that makes the main contribution to the resistance of the structure. In the theoretical analysis, the M interlayer is represented as a multilayer structure with collinear directions of magnetization in the layers.



**Fig. 2.** X-ray $2\theta-\omega$ spectra and rocking curves ($\omega$ scan) of CSCO films ($x = 0.15$) with a thickness of $d_M = 50$ nm deposited on NGO substrates (top). The $2\theta-\omega$ spectrum for the CSCO/YBCO/NGO heterostructure ($d_M = 100$ nm) (bottom).

$Ca_{1-x}Sr_xCuO_2$ (CSCO) film, which is an antiferromagnet with a Néel temperature of several kelvin [13].

The model of the S'/I/AF/S structure is studied theoretically (I is a low-transparency barrier); in this model, the AF structure is treated as one consisting of series-connected ferromagnetic layers (whose planes are oriented perpendicular to the direction of the current) with alternating antiparallel directions of magnetization. The experimental results and theoretical analysis of the proximity effect in these heterojunctions are considered taking into account a barrier between the antiferromagnet and the superconductor.

## 2. EXPERIMENTAL TECHNIQUE

One of the electrodes of the Nb/Au/M/YBCO heterojunctions was made of the S' superconductor with a bilayer structure consisting of niobium (Nb) films with superconducting transition temperature $T_c'' = 9$ K and gold (Au). The proximity effect between the superconductor and metal films (Nb/Au bilayer) ensured the superconducting transition temperature $T_c' = 8-8.5$ of the bilayer. The second electrode of the heterojunction was prepared from a YBCO superconducting cuprate epitaxial film with superconducting transition temperature $T_c = 88-89$ K. The M interlayer was a thin ($d_M = 10-80$ nm) $Ca_{1-x}Sr_xCuO_2$ film (with $x = 0.5$ or $0.15$), viz., AF material [13, 14]. The CSCO/YBCO epitaxial heterostructure was prepared in situ by laser ablation at $T = 800°C$ on a neodymium gallate ($NdGaO_3$, NGO) substrate. In most structures used in the experiment, (110) NGO substrates were used on which growth $c$-oriented [001] YBCO films and, accordingly, CSCO/YBCO heterostructures ensured the transport of electric current in the $c$ direction. Tilting of the crystallographic plane (7 10 2) orientation of the NGO substrate was also used for preparing heterojunctions in which current transport took place predominantly in the [110] direction of YBCO. After preparation of the CSCO/YBCO het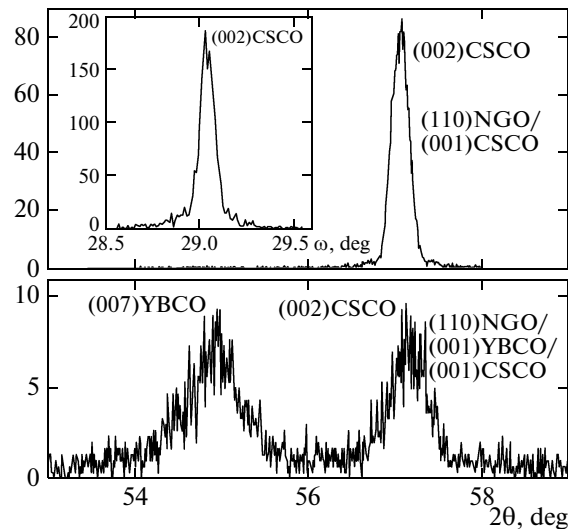erostructure and its cooling without vacuum break, a protecting Au film was deposited to suppress diffusion of oxygen from CSCO/YBCO. The next Nb layer and the additional Au sublayer were deposited by magnetron sputtering with preliminary plasma cleaning of the surface of the initial Au layer. The structure topology was formed using photolithography as well as plasmochemical and ion-beam etching [4, 5, 15]. The structure had the shape of a square with a linear size of $L = 10-50$ μm. As a result, we obtained structures with an AF interlayer, viz., S'/I/AF/S heterojunctions in which the Au/CSCO interface plays the role of the I barrier (see Fig. 1). Nb/Au/YBCO heterojunctions without an AF interlayer were prepared and tested analogously for comparison. Measurements in all types of heterojunctions were taken under identical conditions.

Figure 2 (top) shows the X-ray $2\theta-\omega$ spectra and rocking curves for autonomous epitaxial CSCO films with $x = 0.15$ and $d_M = 50$ nm, deposited on NGO substrates. The results of X-ray diffraction analysis of the CSCO/YBCO heterostructure ($d_M = 100$ nm) are shown in the bottom part of Fig. 2. It can be seen that the width $\Delta(2\theta)$ of the (002) peak of the $2\theta-\omega$ scan of the autonomous CSCO film deposited on the NGO substrate is smaller than $\Delta(2\theta)$ for the CSCO film in the CSCO/YBCO heterostructure and is close to $\Delta(2\theta)$ of the YBCO film. The results of comparison of the lattice constants of CSCO films in the CSCO/YBCO heterostructure and autonomous CSCO films are given in Table 1. It can be seen that the deposition of CSCO onto YBCO slightly deteriorates the quality of CSCO films (the width $\Delta\omega$ of the rocking curve increases) and slightly changes the lattice constants. No other phases differing from autonomous

**Table 1.** Crystallographic parameters of autonomous CSCO films and CSCO/YBCO heterostructures deposited on NGO substrates

| Structure | CSCO | CSCO/YBCO | | CSCO | CSCO/YBCO | |
|---|---|---|---|---|---|---|
| | $x = 0.15$ | $x = 0.15$ | | $x = 0.5$ | $x = 0.5$ | |
| Peak | (002) | (002) | (007) | (002) | (002) | (007) |
| | CSCO | CSCO | YBCO | CSCO | CSCO | YBCO |
| $a_\perp$, nm | 0.321 | 0.322 | 1.169 | 0.334 | 0.336 | 1.177 |
| $\Delta\omega$ | 0.07° | 0.2°* | 0.2°* | 0.4° | 0.5°* | 0.5°* |

Note: Asterisks mark estimates of the rocking curve from the $2\theta-\omega$ scan.

CSCO in chemical composition and orientation were observed.

## 3. RESISTIVITY MEASUREMENTS

At $T > T_c$, the temperature dependence $R(T)$ of the heterojunction resistance is determined by the resistance of the YBCO film due to its high resistivity at $T > T_c$, which exceeds the total contribution of the remaining layers and their interfaces. In the temperature range $T'_c < T < T_c$, the resistance of the YBCO film is zero, and $R(T)$ for heterojunctions with $d_M \leq$ 50 nm exhibited a weak dependence on temperature and was determined by the sum of the resistances of CSCO/YBCO, Au/CSCO, and Nb/Au interfaces, as well as conducting Nb films and the AF interlayer of CSCO (Fig. 3). The resistivity of the Nb/Au interface proved to be low ($\rho \sim 10^{-12}\ \Omega\ cm^2$), which makes a contribution to total resistance $R$ of the heterojunction



**Fig. 3.** Temperature dependence of resistance: *1*—no. 612 sample, $d_M = 20$ nm, $L^2 = 10 \times 10\ \mu m^2$; *2*—no. 610 sample, $d_M = 40$ nm, $L^2 = 50 \times 50\ \mu m^2$; *3*—$\rho d_M/L^2$ ($\rho$ is the resistivity) for an autonomous $Ca_{0.5}Sr_{0.5}CuO_2$ film deposited on the NGO substrate, $d_M = 40$ nm, $L^2 = 50 \times 50\ \mu m^2$.

less than $10^{-6}\ \Omega$ [16]. Taking into account the epitaxial growth of the CSCO/YBCO structure and close values of the Fermi velocity in the components, we can assume that resistance $R_{CSCO/YBCO}$ of the interface is low as compared to the resistance of the Au/CSCO interface, for which the difference in the Fermi velocities of Au and CSCO is significant. Resistivity measurements in autonomous CSCO films with $x = 0.5$ deposited on NGO substrates resulted in high values of resistivity $\rho = 10^3 - 10^4\ \Omega\ cm^2$ at low temperatures [14], which gives a contribution to the resistance of the heterojunction of more than 1 k$\Omega$. It should be noted that the $\rho(T)$ dependence for autonomous CSCO films are typical of systems with hopping conductivities, in which $\ln(\rho) = \ln(\rho_0) + (T_0/T)^{1/4}$ ($\rho_0$ and $T_0$ are experimental constants and the exponent is determined by the dimensionality of the system and corresponds to variable range 3D hopping conductivity in our case). However, the $R(T)$ dependences for heterojunctions with small interlayer thicknesses $d_M < 50$ nm do not exhibit an increase in resistance with decreasing $T$ in the temperature range $T < T_c$, which was observed for autonomous CSCO films. It can be seen from Fig. 3 that the resistances of heterojunctions (curves *1* and *2*) weakly depend on temperature and are much lower than the resistance of the CSCO interlayer (curve *3*) obtained from the calculation based on the resistivity of the autonomous CSCO film. It was shown in [9] that in spite of weak (on the order of one to two atomic cells) cation diffusion at the interface between cuprates, superconductivity may appear at the metal–insulator interface in cuprates due to electron rearrangement or nonstoichiometry in oxygen. Theoretical analysis of the boundary of a strongly correlated Mott insulator shows [17, 18] that charge percolation from one region to another causes a considerable rearrangement in the electron subsystem, which in particular leads to metal-type conductivity (most likely, this effect is observed in our case). At the same time, we cannot rule out that transition of thin ($d_M < 50$ nm) CSCO layers to the metal state may be due to oxygen nonstoichiometry of the boundary layer [19], which was observed in [18] upon an increase in the oxygen concentration in growing CSCO films. Due to the
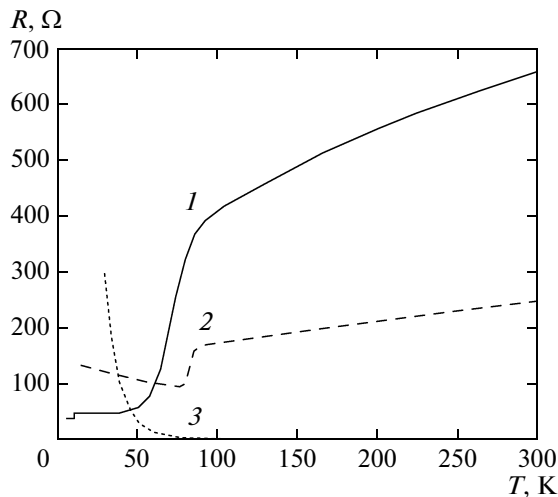
interaction of boundary oxygen atoms in the CSCO film with the YBCO surface in the heterojunctions studied here, the electron conductivity of thin layers in the CSCO interlayer may change substantially, leading to the observed $d_M$ dependence of the heterojunctions in the interval of $T < T_c$. As a result, for $d_M < 50$ nm, the resistance of heterojunctions is mainly determined by the resistance of the Au/CSCO interface. The contribution of the resistance of the CSCO interlayer is substantial for higher values of $d_M > 50$ nm (see Fig. 3); however, the critical current is strongly suppressed in this case.

The characteristic resistance $R_N S$ of heterojunctions ($S = L^2$ is the heterojunction area) measured at $T = 4.2$ K increases exponentially with $d_M$ (Fig. 4). If the main contribution to $R_N S$ comes from the interlayer, we would observe the linear growth with $d_M$ shown by the dotted curve in Fig. 4. The exponential dependence $R_N S(d_M)$ may be due to modification of the electric parameters (conductivity) of the CSCO interlayer due to oxygen nonstoichiometry of thin ($d_M < 50$ nm) films [18, 19] or rearrangement of the electron subsystem of the $M$ interlayer [17, 18]. It follows from experimental data that the doping level in CSCO at the interface with Au is an exponential function of the distance to the source of doping of the YBCO film, which is typical of diffusion processes. Analysis of the electrical conductivity of heterojunctions at high voltages (up to 100 mV) indicates that their $\sigma(V)$ dependences differ from the dependence typical of superconducting contacts with direct conductivity and are rather close to the dependence typical of tunnel-type junctions (probably, due to a low transparency of the Au/Ca$_{1-x}$Sr$_x$CuO$_2$ interface).

## 4. CRITICAL CURRENT

Temperature dependences $I_c(T)$ of the structure with $d_M < 50$ nm follows the temperature dependence of superconducting parameter $\Delta_{Nb}$ in the Nb film for structures without AF interlayers [15]. It is noteworthy that no quadratic increase in the critical current with decreasing temperature, which is typical of SNS structures, is observed in this case [20]. We did not observe the dependence of the characteristic voltage $V_c = I_c R_N$
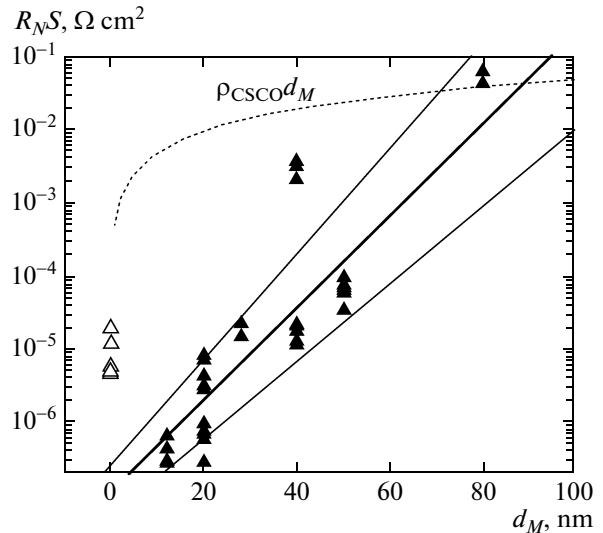


**Fig. 4.** Dependence of characteristic resistance $R_N S$ of heterojunctions on interlayer thickness $d_M$ (▲). Resistance of heterojunctions without M interlayer (△). The bold line shows the exponential dependence $R_N S(d_M)$ with a characteristic growth length of $6 \pm 1$ nm, obtained from statistical processing of experimental data. Fine lines show the error in determining the characteristic length. The dotted curve is the product of resistivity $\rho_{CSCO}$ of the M interlayer, which was determined from measurements on an autonomous film, by thickness $d_M$.

of the structure ($I_c$ is the critical current and $R_N$ is the normal resistance of the heterojunctions) on the thickness of the CSCO interlayer either (see Table 2). It should be noted that in all heterojunctions studied here with a critical current $I_c > 1$ μA, thickness $d_M$ amounts to tens of nanometers; i.e., the penetration depth of superconducting correlations in CSCO considerably exceeds the coherence length of the FeMn polycrystalline AF interlayer, which constitutes a few nanometers [21]. The penetration depth for superconducting correlations in CSCO can be estimated from the measurements of the $j_c(d_M)$ dependence of the superconducting current density on the thickness. Figure 5 shows such experimental data. Statistical processing of the $j_c(d_s)$ dependence gives the decay depth of the superconducting wavefunction $\xi_{AF} = 7 \pm 1$ nm.

**Table 2.** Electrophysical parameters of heterostructures at $T = 4.2$ K

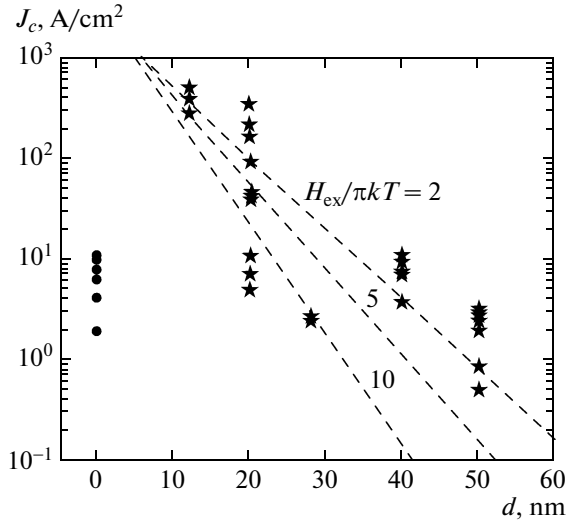| Sample no. | Tilt angle of substrate | $x$ | $d_M$, nm | $L$, μm | $I_c$, μA | $R_N$, Ω | $C$, pF | $q$ |
|---|---|---|---|---|---|---|---|---|
| 269 | 0 | 0.15 | 50 | 10 | 44 | 3.4 | 0.65 | 0.2 |
| 271 | 0 | 0.15 | 20 | 10 | 50 | 1.9 | 1.9 | 0.08 |
| 273 | 11° | 0.5 | 20 | 10 | 335 | 0.8 | 2 | 0.3 |
| 274 | 11° | 0.5 | 50 | 10 | 2.5 | 60 | 0.06 | 0.13 |
| 610 | 0 | 0.5 | 40 | 50 | 0.6 | 93 | – | – |
| 612 | 0 | 0.5 | 12 | 10 | 202 | 1.73 | 0.55 | – |

$J_c$, A/cm$^2$



**Fig. 5.** Experimental results on the dependence of the superconducting current density on $d_M$ for heterostructures with a CSCO interlayer with doping level of $x = 0.5$ (★) and for heterostructures without the M interlayer (●). Dashed lines show the theoretical dependences of the critical current on the thickness of the AF interlayer for three values of normalized exchange field $H_{ex}/\pi kT = 2$, 5, and 10. Theoretical dependences are the normalized critical current density choosing interlayer thickness in accordance with the condition of best matching of the theory to experiment ($\xi_{AF} = 10$ nm).

## 5. THEORETICAL MODEL

To confirm some of the experimental results and analyze the qualitative features of the proximity effect in the heterostructures studied here, let us consider a model of the S'/I/M/S structure with a magnetic multilayer M located between two superconductors S and S' (see Fig. 1). In this model, we assume that the M interlayer consists of metallic ferromagnetic (F) layers with a thickness $d$ much larger than the atomic spacing and that the exchange field $H_{ex}$ with antiparallel (or parallel) orientations in adjacent layers lies in the plane of these layers. We also assume that exchange field $H_{ex}$ is much smaller than the Fermi energy. In our calculations, we suppose that S and S' superconductors exhibit the $s$ type of superconducting pairing.[1]

The model considered here can be analyzed using the semiclassical equations for the Green functions (see, for example, [1, 2]). We will also assume that conditions are realized in which the superconducting condensate wavefunction in the region of ferromagnetic layers can be treated as small (this is observed for transparency of the M/S boundary that is much smaller than unity at all temperatures or for an arbitrary transparency of the M/S boundary at a temperature close to the superconducting transition tempera-

ture $T_c$). The transparency of the barrier associated with the I barrier is regarded as smaller than the transparency of the M/S interface; consequently, the effect of superconductor S' on the condensate function in the M interlayer can be disregarded. In the case under investigation, the condensate Green function has two components, $f_\sigma$ ($\sigma = \pm 1$), corresponding to opposite spin orientations. Let us analyze the "dirty limit" in which mean free path $l$ is much smaller than the layer thickness and, in addition, $\tau H_{ex} \ll 1$, where $\tau$ is the time of scattering from impurities. In this case, the isotropic part of Green function $\langle f_\sigma \rangle = s_\sigma \gg f_\sigma - s_\sigma$ satisfies a wave-type equation ($s_\sigma \ll 1$)

$$\partial_{xx}^2 s_\sigma - k_\sigma^2 s_\sigma = 0, \qquad (1)$$

in which

$$k_\sigma = [2(\omega + i\sigma H_{ex}(x))/D]^{1/2}, \qquad (2)$$

where $D$ is the diffusion coefficient in the F layers and $\omega = \pi T(2m + 1)$ is the Matsubara frequency (we assume that $\omega > 0$). In the case of AF ordering in the layers, the solution for $s_\sigma$ for $0 < x < d_M = Nd$ ($N$ is the number of ferromagnetic layers) can be written in the form

$$s_\sigma(x) = \begin{cases} A_n^\sigma \cosh k_\sigma(x - x_{n-1}) + B_n^\sigma \sinh k_\sigma(x - x_{n-1}) \\ x_{n-1} < x < x_n, \\ A_{n+1}^\sigma \cosh k_{-\sigma}(x - x_n) \\ + B_{n+1}^\sigma \sinh k_{-\sigma}(x - x_n), \quad x_n < x < x_{n+1}, \end{cases} \qquad (3)$$

where $x_n = nd$. Taking into account the continuity of function $s_\sigma$ and its derivatives for $x = x_n$, we can obtain the following recurrence relation for the coefficients:

$$\begin{pmatrix} A_{n+1}^\sigma \\ B_{n+1}^\sigma \end{pmatrix} = \mathbf{M}_{\sigma_n} \begin{pmatrix} A_n^\sigma \\ B_n^\sigma \end{pmatrix}, \qquad (4)$$

in which matrix $\mathbf{M}_\sigma$ is defined as

$$\mathbf{M}_\sigma = \begin{pmatrix} 1 & 0 \\ 0 & q_\sigma \end{pmatrix} \begin{pmatrix} \cosh\lambda_\sigma & \sinh\lambda_\sigma \\ \sinh\lambda_\sigma & \cosh\lambda_\sigma \end{pmatrix}, \qquad (5)$$

where $q_\sigma = [(\omega + i\sigma H_{ex})/(\omega - i\sigma H_{ex})]^{1/2}$, $\lambda_\sigma = k_\sigma d$, and $\sigma_n = (-1)^{n+1}\sigma$. Taking into account the boundary condition for $x = 0$, $\partial_x s_\sigma(0) = 0$, we obtain $B_1^\sigma = 0$. Consequently, introducing the notation

$$\prod_{n=1}^{N-1} \mathbf{M}_{\sigma_n} = \|m_\sigma^{ij}\|, \qquad (6)$$

we obtain an expression that follows from formulas (4) and (5) and defines the relation between the values of (symmetric) condensate function for $x = 0$ and $x = d_M$:

$$s_\sigma(0) = c_\sigma s_\sigma(d_M), \qquad (7)$$

---

[1] In this section, to simplify calculations, we assume that Boltzmann constant $k$ and Planck constant $\hbar$ are equal to unity.

where

$$c_\sigma = \frac{1}{m_{\sigma_N}^{11}\cosh\lambda_{\sigma_N} + m_{\sigma_N}^{21}\sinh\lambda_{\sigma_N}}.$$

Function $c_\sigma$ connecting the values of the condensate function at the opposite edges of the M interlayer describes the evolution of the condensate Green function in the M structure. Analysis of this function shows that in the case of AF ordering of the magnetization in the M interlayer, the condensate Green function can penetrate into the M layer to a depth on the order of $\xi_N = (D/\pi T)^{1/2}$ even if $\xi_H = (D/\pi H_{ex})^{1/2} \ll \xi_N$, where $\xi_H$ is the penetration depth for the condensate function in the case of ferromagnetic ordering of magnetization in the layers. Such a situation is realized when the condition $d = d_M \ll \xi_H$ holds. For a fixed thickness of the AF interlayer, the proximity effect becomes stronger upon an increase in the number of layers [22]. Thus, in contrast to ferromagnetic ordering, anomalous long-range proximity effect (LRPE) may take place in the case of AF ordering of magnetization in the layers. In contrast to the LRPE predicted in [23] and associated with the emergence of the triplet component of the condensate Green function, which is observed in the case of noncollinear spatially nonuniform magnetization in ferromagnets, the LRPE considered here is associated with the singlet component of the condensate Green function. The triplet component decaying in the M interlayer over the same length as the singlet component makes zero contribution to the Josephson current in the structure considered here. Manifestations of the LRPE and other features of the proximity effect in various weak links including structures with an M multilayer with the AF ordering of magnetization were analyzed by one of the authors in [22, 24] and by the authors of [25, 26].

Let us consider LRPE manifestations in structures of the S'/I/M/S type. The expression for the Josephson current in such a structure with a low-transparency barrier, which determines the resistance of the structure in the normal state, has the conventional form $I = I_c\sin\varphi$, where $I_c(H_{ex})$ is defined by the formula

$$\frac{I_c}{I_{c0}} = \frac{F(H_{ex})}{F(0)} \equiv i_c(H_{ex}), \qquad (8)$$

where

$$F(H_{ex}) = \mathrm{Re}\sum_{n=0}^{\infty} s_+(0)f_{S'},$$

$f_{S'}$ is the condensate function of superconductor S', and $I_{c0}$ is the value of the critical current in the structure with a normal interlayer (S'/I/N/S) and with the same parameters (thickness, mean free path, and so on) as in the M interlayer.

Let us now consider a pure interlayer in which the mean free path exceeds the thickness. In this case, the condensate function in the M interlayer obeys the Eilenberger equation (see, for example, [2]), which can be used to obtain the relation

$$i_c(H_{ex}) = \frac{W(\overline{H}_{ex})}{W(0)},$$

where

$$W(\overline{H}_{ex})$$
$$= \sum_{m=0}^{\infty} f_{S'} \int_{-1}^{1} \overline{D}\,\mathrm{Re}f(\omega + i\overline{H}_{ex}, \mu, x = 0)|\mu|d\mu,$$

$\mu = \cos\theta$, $\theta$ being the angle between the direction of the momentum and the $x$ axis; $f(\omega, \mu, x)$ is the condensate Green function in the case of a normal interlayer; $\overline{D}$ is the transparency of the I barrier, and $\overline{H}_{ex} = H_{ex}/N$ for an odd number $N$ of the layers and $\overline{H}_{ex} = 0$ for an even number $N$. Thus, in the clean limit, $i_c(H_{ex}) = W(H_{ex}/N)/W(0)$ for odd $N$ and $i_c(H_{ex}) = 1$ for even $N$. The characteristic depth at which the amplitude of function $W(\overline{H}_{ex})$ (as well as of function $W(0)$) decreases exponentially with increasing $d_M$ is determined by the value of coherence length for clean limit $\xi_N = v_F/\pi T$ (for $\tau T \gg 1$).

## 6. DISCUSSION

Figure 5 shows the theoretical dependences (dashed curves) for $j_c$ corresponding to three values of normalized exchange field $H_{ex}/\pi kT$ in the F layers of the S'/I/M/S structure with an AF interlayer ($N = 20$), which were obtained for $\xi_{AF} = 10$ nm. The theoretical dependences are given for a low transparency of the M/S interface (exceeding the transparency of the I barrier) and identical S and S' superconductors. It should be noted that the form of the theoretical $j_c(d_M)$ dependences does not change qualitatively in the case of different superconductors. In our experiment, the superconductors are not identical; moreover, the condensate function with the $s$ symmetry in YBCO is not a dominant function. However, for the normalized values of $j_c(d_M)$ shown in Fig. 5, the condensate Green function for the electrodes does not play an important role and the normalization of theoretical dependences (for $\xi_{AF} = 10$ nm) was chosen from the condition of best matching between experiment and theory. It can be seen that the theoretical dependence $j_c(d_M)$ for $H_{ex}/\pi kT = 2$ describes the experimental data more correctly than the dependences obtained for higher values of $H_{ex}/\pi kT$. With increasing exchange field $H_{ex}$, the value of $j_c$ decreases and the difference between the values of $j_c$ corresponding to even and odd number of F layers becomes more significant. It should be recalled that the radical difference between the Josephson current in S/AF/S junctions with even and odd numbers of layers was predicted earlier in [12], in which the model of an antiferromagnet with atomically thin layers was analyzed. The structures contain-
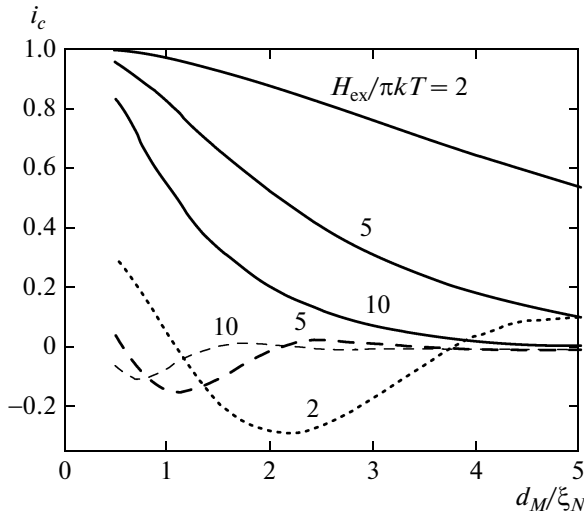
**Fig. 6.** Theoretical dependences of normalized critical current $i_c$ on normalized thickness $d_M/\xi_N$ of the M interlayer for three values of normalized exchange field $H_{ex}/\pi kT$. Solid curves correspond to the AF interlayer, while dashed curves correspond to the F interlayer.

ing an arbitrary number of ferromagnetic layers (with a thickness much larger than atomic spacing) with AF ordering of magnetization (in particular, the dependence of transport properties on the number of layers) were analyzed in [22].

Figure 6 shows the theoretical dependences of normalized critical current $i_c(d_M)$ (8) of heterojunctions with AF and F ordering of magnetization in the M interlayer. The critical current is normalized to the value of $I_{c0}$ observed in S'/I/N/S structures. It can be seen from Fig. 6 that in the case of the F interlayer, a stronger decrease in the value of $i_c$ is observed upon an increase in the thickness of the M interlayer, and the shape of the $i_c(d_M)$ curves changes qualitatively. In particular, an increase in $d_M$ may induce a transition between the 0 and $\pi$ states of the heterojunctions under investigation. Such a transition was observed in experiments with S/F/S junctions with a single-layer F barrier [27]. Note that for our heterojunctions, the condition of the smallness of the thickness $d = d_M/N \ll \xi_H$ of a layer in the M interlayer is a necessary condition for the LRPE [22].

In experiments, the oscillating (containing zero minima) dependence of the critical current in heterojunctions on the external magnetic field [28] and the preserved symmetry of the current–voltage characteristics ($I$–$V$ curves) indicate the homogeneity of the M interlayer. To verify the correspondence of manifestation of the nonstationary Josephson effect to the RSJ model criteria [10], we analyzed the $I$–$V$ characteristics of heterojunctions under microwave radiation and the behavior of the selective detector response $\eta(V)$. We detected multiple oscillations of the critical current and Shapiro steps; the maximal values of the first

Shapiro step approached the theoretical maximum upon an increase in the normalized frequency $f_e/f_c$ of microwave radiation, where $f_c = (2e/h)I_c R_N$. At the same time, a discrepancy with the RSJ model (in particular, the formation of fractional Shapiro steps) was observed. It is well known [29, 30] that the mixed ($d$ and $s$) symmetry of the order parameter of one of the electrodes in the heterojunction facilitates the generation of the second harmonic in the dependence of the superconducting current on the phase difference of the waves functions of the electrodes (current–phase relation, CPR). To find the deviation of this dependence from a sinusoid, we used the method developed earlier and based on the measurement of the amplitudes of the Shapiro steps emerging as a result of synchronization of intrinsic Josephson generation by an external monochromatic microwave signal at frequency $f_e$ [15]. In the presence of the second harmonic on the CPR, fractional Shapiro steps appear in additional to integer Shapiro steps on the $I$–$V$ curve for $V_n = n(h/2e)f_e$; in particular, for $n = 1/2$, such steps are formed for voltage $V_{1/2} = (1/2)V_1$. The experimental dependences of the critical current and of the integer and fractional steps on the microwave current were compared with the results of calculation based on a modified RSJ model of a Josephson junction taking into account the second harmonic on the CPR and the capacitance of the heterostructure [15]. The fraction of the second harmonic defined by quantity $|q| = I_{c2}/I_{c1}$, where $I_{c1}$ and $I_{c2}$ are the amplitudes of the first and second CPR harmonics, was determined as a free parameter. The sign of $q$ was found from comparison of the calculated values with the experimental results for the fractional step ($I_{1/2}$). The values of $q$ and electrophysical parameters of the structures are given in Table 2. The deviation of the CPR from a sinusoid are also confirmed by the detector response measurements taken under a weak external action of an electromagnetic field with a power $P$ on the order of several picowatts, which ruled out the formation of fractional Shapiro steps as a result of external pumping. The presence of the second harmonic in the CPR of the Josephson junction leads to the emergence of a subharmonic selective detector response $\eta_{1/2}(V)$ with peaks at $V = V_{1/2} \pm \delta V$, where $\delta V$ is the halfwidth of the second harmonic of Josephson generation at frequency $f_2 = 2(2e/h)V_{1/2}$. The estimates of the weight of the CPR second harmonic obtained in this way using the formula $|q| \approx 0.5(_{max}\eta_1/_{max}\eta_2)^{1/2}$ [15] resulted in values close to those obtained from analysis of the oscillatory dependences of Shapiro steps. Figure 7 shows the experimental dependence of the detector response, which contains the fundamental and subharmonic peaks. The inset shows the linear dependence of the amplitude of detector responses on power $P$ of the field, corresponding to the quadratic detection mode observed in the case of a weak external action.
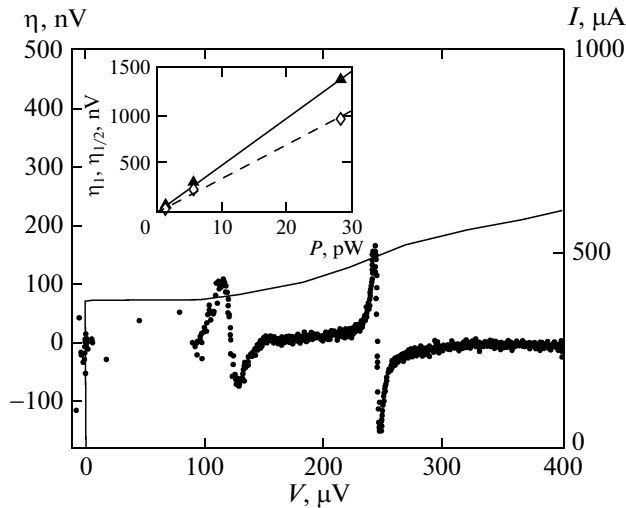
**Fig. 7.** Current−voltage characteristic of heterojunctions (solid curve) and detector response to electromagnetic radiation of frequency 119.5 GHz (dots). The inset shows the dependences of the main response for $V_1 = 246$ μV on the microwave power (triangles) and fractional response for $V_{1/2} = 123$ μV (rhombs).

## 7. CONCLUSIONS

In experiments with $Nb/Au/Ca_{1-x}Sr_xCuO_2/YBa_2Cu_3O_{7-\delta}$ hybrid superconducting structures with an AF interlayer of thickness from 10 to 50 nm, a superconducting current of Josephson nature is observed. The theoretical model of the superconducting junction containing a multilayer AF structure with collinear orientation of magnetization in the F layers is analyzed. It is shown experimentally and theoretically that such structures exhibit an anomalously strong proximity effect responsible for the manifestation of the Josephson effect. The experimental data obtained from measuring the magnetic-field characteristics of the critical current and the characteristics of the nonstationary Josephson effect in the millimeter frequency range, including detector response to a weak external action, rule out the presence of pinholes and the percolation mechanism of current flow. The deviation of the CPR from the sinusoidal dependence following from microwave measurements using ultraweak picowatt signals, which is observed for heterojunctions with and without an AF interlayer, can be explained by the presence of the electrode made of a cuprate superconductor with a dominant $d$-wave component of the order parameter.

## ACKNOWLEDGMENTS

## REFERENCES

1. A. I. Buzdin, Rev. Mod. Phys. **77**, 935 (2005).

2. F. S. Bergeret, A. F. Volkov, and K. B. Efetov, Rev. Mod. Phys. **77**, 1321 (2005).

3. I. Bozovic, G. Logvenov, M. A. J. Verhoeven, P. Caputo, E. Goldobin, and M. R. Beasley, Phys. Rev. Lett. **93**, 157002 (2004).

4. G. A. Ovsyannikov, I. V. Borisenko, F. V. Komissinskiǐ, Yu. V. Kislinskiǐ, and A. V. Zaǐtsev, Pis'ma Zh. Éksp. Teor. Fiz. **84** (5), 320 (2006) [JETP Lett. **84** (5), 262 (2006)].

5. P. Komissinskiy, G. A. Ovsyannikov, I. V. Borisenko, Yu. V. Kislinskii, K. Y. Constantinian, A. V. Zaitsev, and D. Winkler, Phys. Rev. Lett. **99**, 017004 (2007).

6. Y. Tarutani, T. Fukazawa, U. Kabasawa, A. Tsukamoto, M. Hiratani, and K. Takagi, Appl. Phys. Lett. **58**, 2707 (1991).

7. K.-U. Barholz, M. Yu. Kupriyanov, U. Hübner, F. Schmidl, and P. Seidel, Physica C (Amsterdam) **334**, 175 (2000).

8. V. Kresin, Yu. Ovchinnikov, and S. Wolf, Appl. Phys. Lett. **83**, 722 (2003).

9. A. Gozar, G. Logvenov, L. F. Kourkoutis, A. T. Bollinger, L. A. Giannuzzi, D. A. Muller, and I. Bozovic, Nature (London) **455**, 782 (2008).

10. A. Barone and G. Paterno, *Physics and Applications of the Josephson Effect* (Wiley, New York, 1982; Mir, Moscow, 1984).

11. L. P. Gorkov and V. Z. Kresin, Physica C (Amsterdam) **103** (2002).

12. B. M. Andersen, I. V. Bobkova, P. J. Hirschfeld, and Yu. S. Barash, Phys. Rev. Lett. **96**, 117005 (2006).

13. D. Vaknin, E. Caignol, P. K. Davies, J. E. Fischer, D. C. Johnston, and D. P. Goshorn, Phys. Rev. B: Condens. Matter **39**, 9122 (1989).

14. G. A. Ovsyannikov, S. A. Denisyuk, and I. K. Bdikin, Fiz. Tverd. Tela (St. Petersburg) **47** (3), 417 (2005) [Phys. Solid State **47** (3), 429 (2005)].

15. P. Komissinskiy, G. A. Ovsyannikov, K. Y. Constantinian, Y. V. Kislinski, I. V. Borisenko, I. I. Soloviev, V. K. Kornev, E. Goldobin, and D. Winkler, Phys. Rev. B: Condens. Matter **78**, 024 501 (2008).

16. F. V. Komissinski, G. A. Ovsyannikov, Yu. V. Kislinskiǐ, I. M. Kotelyanskiǐ, and Z. G. Ivanov, Zh. Éksp. Teor. Fiz. **122** (6), 1247 (2002) [JETP **95** (6), 1074 (2002)].

17. S. Okamoto and A. J. Millis, Nature (London) **428**, 630 (2004).

18. J. C. Nie, P. Badica, M. Hirai, Y. Kodama, A. Crisan, A. Sundaresan, Y. Tanaka, and H. Ihara, Physica C (Amsterdam) **388**−**389**, 441 (2003).

19. S. J. L. Billinge, P. K. Davies, T. Egami, and C. R. A. Catlow, Phys. Rev. B: Condens. Matter **43**, 10 340 (1991).

20. K. A. Delin and A. W. Kleinsasser, Supercond. Sci. Technol. **9**, 227 (1996).

21. C. Bell, E. J. Tarte, G. Burnell, C. W. Leung, D.-J. Kang, and M. G. Blamire, Phys. Rev. B: Condens. Matter **68**, 144 517 (2003).

22. A. V. Zaitsev, Pis'ma Zh. Éksp. Teor. Fiz. **90** (6), 521 (2009) [JETP Lett. **90** (6), 475 (2009)].

23. A. F. Volkov, F. S. Bergeret, and K. B. Efetov, Phys. Rev. Lett. **90**, 117 006 (2006).

24. A. V. Zaitsev, Pis'ma Zh. Éksp. Teor. Fiz. **83** (6), 277 (2006) [JETP Lett. **83** (6), 233 (2006)]; Pis'ma Zh. Éksp. Teor. Fiz. **88** (7), 521 (2008) [JETP Lett. **88** (7), 448 (2008)].

25. T. Yu. Karminskaya and M. Yu. Kupriyanov, Pis'ma Zh. Éksp. Teor. Fiz. **86** (1), 65 (2007) [JETP Lett. **86** (1), 61 (2007)].

26. B. Crouzy, S. Tollis, and D. A. Ivanov, Phys. Rev. B: Condens. Matter **76**, 134 502 (2007).

27. V. V. Ryazanov, V. A. Oboznov, A. Yu. Rusanov, A. V. Veretennikov, A. A. Golubov, and J. Aarts, Phys. Rev. Lett. **86**, 2427 (2001); J. Low Temp. Phys. **136**, 385 (2004).

28. Yu. V. Kislinskii, P. V. Komissinski, K. Y. Constantinian, G. A. Ovsyannikov, T. Yu. Karminskaya, I. I. Soloviev, and V. K. Kornev, Zh. Éksp. Teor. Fiz. **128** (3), 575 (2005) [JETP **101** (3), 494 (2005)].

29. A. A. Golubov, M. Yu. Kupriyanov, and E. Il'ichev, Rev. Mod. Phys. **76**, 411 (2004).

30. P. V. Komissinski, E. Il'ichev, G. A. Ovsyannikov, S. A. Kovtonyuk, M. Grajcar, R. Hlubina, Z. Ivanov, Y. Tanaka, N. Yoshida, and S. Kashiwaya, Europhys. Lett. **57**, 585 (2002).

*Translated by N. Wadhwa*